Magnetic interactions in disordered perovskite $PbFe_{1/2}Nb_{1/2}O_3$ and related compounds: Dominance of nearest-neighbor interaction

R. O. Kuzian,[1,2] I. V. Kondakova,[1] A. M. Daré,[3] and V. V. Laguta[1,4]
[1]*Institute for Problems of Materials Science NASU, Krzhizhanovskogo 3, 03180 Kiev, Ukraine*
[2]*Donostia International Physics Center (DIPC), ES-20018 Donostia-San Sebastian, Spain*
[3]*Aix-Marseille Université, CNRS, IM2NP UMR 7334, F-13397, Marseille, France*
[4]*Institute of Physics, AS CR, Cukrovarnicka 10, 16253 Prague, Czech Republic*
(Received 29 July 2013; revised manuscript received 26 November 2013; published 6 January 2014)

We show that the magnetism of double perovskite $AFe_{1/2}M_{1/2}O_3$ systems may be described by the Heisenberg model on the simple cubic lattice, where only half of sites are occupied by localized magnetic moments. The nearest-neighbor interaction J_1 is more than 20 times the next-nearest-neighbor interaction J_2, the third-nearest interaction along the space diagonal of the cube being negligible. We argue that the variety of magnetic properties observed in different systems is connected with the variety of chemical ordering in them. We analyze six possible types of the chemical ordering in a $2 \times 2 \times 2$ supercell, and argue that the probability to find them in a real compound does not correspond to a random occupation of lattice sites by magnetic ions. The exchange J_2 rather than J_1 define the magnetic energy scale of most double perovskite compounds that means the enhanced probability of 1:1 short-range ordering. Two multiferroic compounds $PbFe_{1/2}M_{1/2}O_3$ (M = Nb, Ta) are exceptions. We show that the relatively high temperature of the antiferromagnetic transition is compatible with a layered short-range chemical order, which was recently shown to be most stable for these two compounds [I. P. Raevski *et al.*, Phys. Rev. B **85**, 224412 (2012)]. We show also that one of the types of ordering has a ferrimagnetic ground state. The clusters with a short-range order of this type may be responsible for a room-temperature superparamagnetism, and may form the cluster glass at low temperatures.

DOI: 10.1103/PhysRevB.89.024402 PACS number(s): 75.30.Et, 75.50.Lk

I. INTRODUCTION

The compound $PbFe_{1/2}Nb_{1/2}O_3$ (PFN) is one of the first multiferroics reported [1,2]. It remains to be in focus of the attention of the multiferroic community [3–9]. Despite the long story of studies, the magnetic properties of PFN are not fully understood. It belongs to the family of double perovskites $AFe_{1/2}M_{1/2}O_3 = A_2FeMO_6$ with a nonmagnetic cation in the A site (A = Pb,Ca,Sr,Ba) of the perovskite structure ABO_3 and a distribution of the magnetic Fe^{3+} and nonmagnetic M^{5+} cations (M = Nb,Ta,Sb) in the six-coordinated B site of the structure (see Fig. 1).

The magnetic properties of these compounds are defined by Fe^{3+}, $S = 5/2$ ions that occupy half of the sites of simple cubic lattice (sublattice B of perovskite structure), and interact via various superexchange paths.

It is natural to compare the magnetism of $AFe_{1/2}M_{1/2}O_3$ compounds with ortoferrites $RFeO_3$ (R = Y or a rare earth) and bismuth ferrite $BiFeO_3$, with a similar perovskite structure where Fe occupy every B site. All these compounds exhibit essentially antiferromagnetic ordering (with a small canting of predominantly antiferromagnetic spins) below the transition temperature, which varies in the range $620 < T_N(1) < 740$ K [10–12]. The nearest-neighbor Fe-Fe interaction (via the Fe-O-Fe path) was estimated as $J_1 \sim 50$ K [11,13–18], the next-nearest neighbor being much smaller $\alpha = J_2/J_1 \simeq 0.05$ [13–15].

If one assumes (i) a random occupation of the site B by Fe and M ions (the x-ray diffraction and Mössbauer spectra support this assumption for most of the M ions), and (ii) a similar value of Fe-O-Fe superexchange, we may expect the Néel temperature $T_N(0.5) \sim 0.5T_N(1) > 300$ K. This estimate comes from an analogy with $T_N(x)$ behavior in the disodered perovskite system $KMn_xMg_{1-x}F_3$ [19,20], which agree with theoretical considerations of dilute Heisenberg magnets [21,22]. Contrary to these expectations, most of the $AFe_{1/2}M_{1/2}O_3$ compounds exhibit a magnetic anomaly at $T \sim 25$ K [23,24]. One observes $T_N \sim 150$ K only for $PbFe_{1/2}M_{1/2}O_3$ (M = Nb,Ta) [1]. It seems that at least one of the above assumptions (i) and (ii) is false.

Evidences for partial chemical ordering in the B sublattice comes from experiment [6,23–25] and theory [7,26]. The disorder in the distribution of Fe and M ions was modeled in Refs. [7,27] by a set of six periodic lattices PFB0 . . . PFB5 with the supercell containing $8 = 2 \times 2 \times 2$ perovskite cells with different versions of chemical order (ion distributions) within the cells (see Fig. 2). It was shown that the total energy is different for different configurations [27], and the hierarchy of the energies depends on the type of M ion.

Recent reports on room-temperature multiferroicity of PFN/$PbZr_xTi_{1-x}O_3$ [28], and of related solid solution systems $PbFe_{1/2}Ta_{1/2}O_3$/$PbZr_xTi_{1-x}O_3$ [29,30] and $Pb(Fe_{2/3}W_{1/3})O_3$/$PbZr_xTi_{1-x}O_3$ [31] evidences in favor of the presence in these systems of magnetic interactions J with the energy scale $S(S+1)J/k_B = 8.75J/k_B \sim 300$ K. In Ref. [32], the nearest-, second-, and fourth-nearest-neighbor exchange interactions between Fe^{3+} ions were found from LSDA+U calculations for $PbFe_{1/2}Ta_{1/2}O_3$. The nearest-neighbor exchange occurs [in our notations, see Eq. (1)] to be $J_1/k_B \approx 42$ K; it gives $S(S+1)J/k_B = 366$ K.

In this work, using first-principle calculations, we find the values of exchange interaction between nearest-, second-, and third-nearest-neighbor Fe^{3+} ions in PFN, and confirm the validity of the assumption (ii), i.e., we show that the nearest-neighbor interaction dominates, and its value is close

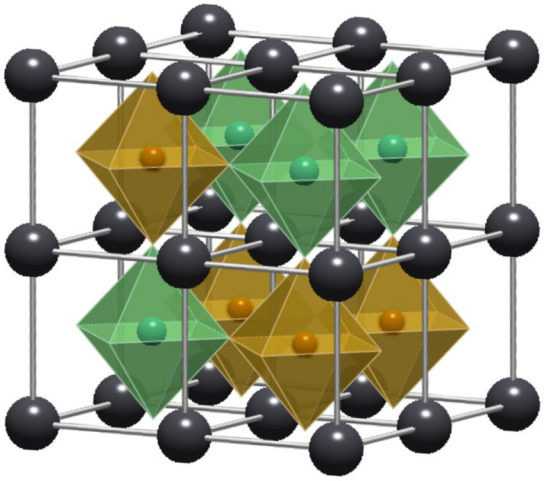

FIG. 1. (Color online) A fragment of disordered $PbFe_{1/2}Nb_{1/2}O_3$ structure. The supercell containing $8 = 2 \times 2 \times 2$ perovskite cells is shown. Black circles denote Pb ions; green (brown) circles inside oxygen octahedra depict Nb (Fe) ions. Oxygen ions are located in the corners of the octahedra. The distribution of Fe and Nb ions corresponds to PFB4 chemical order (see text).

to that found for $RFeO_3$ and $PbFe_{1/2}Ta_{1/2}O_3$ compounds. So, the peculiarities of magnetic properties of $AFe_{1/2}M_{1/2}O_3$ compounds are related with chemical ordering in the B sublattice.

II. METHOD

The density functional theory calculations were performed using the full-potential local-orbital (FPLO) code [33]. We have used the default FPLO basis, which is claimed to be technically complete, i.e., the FPLO code developers have checked the convergence of the electronic density with respect to the number of basis functions for a huge number of compounds, including $3d$-metal oxides. The FPLO basis consists of localized atomiclike functions defined by angular nl-quantum numbers and the number of numerical radial functions per orbital. Each valence state can come as single, double or triple state, which means that there are one, two or three radial basis functions for this nl-quantum number. The default basis for Fe is single 3s3p4p, and double 4s3d; for O, single 1s3d, double 2s2p; for Pb, single 5s5p5d6d, double 6s6p; for Nb, single 4s4p5p and double 5s4d. The exchange and correlation potential of Perdew and Wang [34] was employed as well as the FPLO implementation of the LSDA + U method in the atomic limit scheme [35,36], and parameters $U \equiv F^0 = 4$ and 6. The intra-atomic exchange parameters were fixed at the values $F^2 = 49B + 7C = 10.3$ eV, and $F^4 = 63C/5 = 7.5$ eV, which corresponds to Racah parameters $B = 1015$ cm^{-1}; $C = 4800$ cm^{-1} for free Fe^{3+} ion [37].

The calculations were made for the $2 \times 2 \times 2$ 40 atom supercell $Pb_8Fe_4Nb_4O_{24}$ (symmetry group P1, No. 1) shown schematically in Fig. 1. The $4 \times 4 \times 4$ k mesh was used for the Brillouin zone integration. First, we have defined the magnetic interaction for the cubic perovskite structure that corresponds to the paraelectric phase of PFN with the experimental lattice parameter $a = 4.01$ Å, and PFB4 chemical order (Fig. 3). Then we have checked that the interaction values are essentially the same for all kinds of chemical orders and for actual distorted perovskite structure of PFN. The ion coordinates for all possible types of the chemical ordering shown in Fig. 2 were taken from the results of full relaxation [38] that has been performed in Ref. [7].

The total energies for different structural and magnetic configurations were obtained, and the results were mapped onto an effective Hamiltonian,

$$\hat{H} = E_n + \frac{1}{2}\sum_{\mathbf{R},\mathbf{g}} J_{\mathbf{g}} \hat{\mathbf{S}}_{\mathbf{R}} \hat{\mathbf{S}}_{\mathbf{R}+\mathbf{g}}, \qquad (1)$$

where E_n is a nonmagnetic, spin-independent part of the energy, which depends on chemical configuration [7]. The

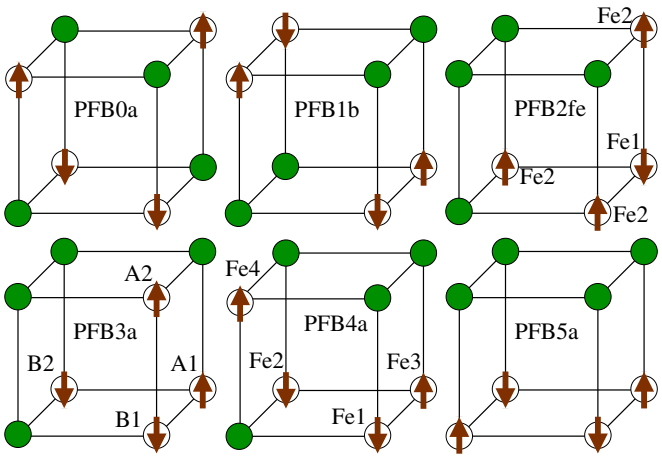

FIG. 2. (Color online) Magnetic ground states for different chemical configurations of Fe^{3+} (open circles) in a $2 \times 2 \times 2$ supercell of $AFe_{1/2}Nb_{1/2}O_3$ (A = Pb,Ba; only B-sublattice sites are shown). Green filled circles denote nonmagnetic Nb^{5+} ions. PFB0a is the I-type order of the fcc lattice.

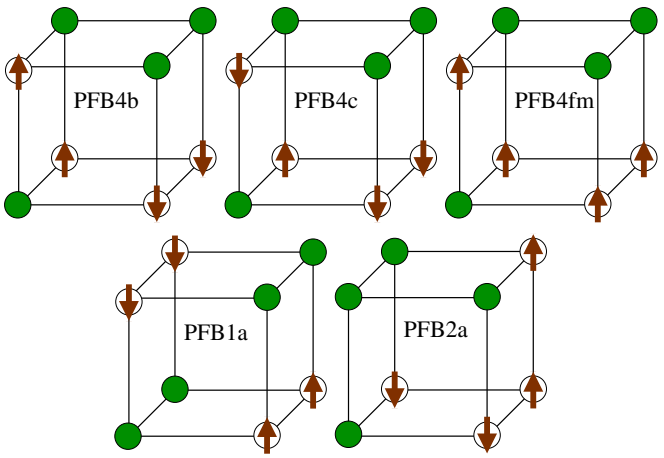

FIG. 3. (Color online) (Upper panel) The excited magnetic states of PFB4 chemical order that were used for the calculations of the interactions. (Lower panel) Additional magnetic structures, which were used for the check of the mapping of LSDA + U on the Heisenberg model (1).

spin-dependent part of the interaction has the form of a Heisenberg term. The sum goes over the lattice sites **R** occupied by magnetic Fe^{3+} ions, vectors **g** join interacting spins. The $2 \times 2 \times 2$ supercell allows one to determine the values of nearest-, second-nearest-, and third-nearest-neighbor interactions J_1, J_2, J_3, which corresponds to sites separated by the edge, face diagonal, and space diagonal of perovskite unit cell. For a given spin configuration, the total energy per supercell is

$$E_c = \langle \hat{H} \rangle = E_n + \frac{1}{2} \sum_{\mathbf{s},\mathbf{g}} J_{\mathbf{g}} \langle \hat{\mathbf{S}}_{\mathbf{s}} \hat{\mathbf{S}}_{\mathbf{s}+\mathbf{g}} \rangle, \tag{2}$$

where **s** is the magnetic ion position within the cell, $\langle \hat{\mathbf{S}}_{\mathbf{s}} \hat{\mathbf{S}}_{\mathbf{s}+\mathbf{g}} \rangle = cS^2$, $c = +1(-1)$ for parallel (antiparallel) spin arrangement.

III. RESULTS

The details concerning the calculated electronic structure of PFN are given in Appendix A. Here we concentrate on the magnetic interactions. The results for the total energy calculations for different spin arrangement in PFB4 chemical order (Figs. 1–3) of ideal cubic perovskite structure are given in Table I. The expressions for the magnetic energy for the considered supercells are given in the second column of Table II. The third column of the table gives the energies that we obtained in LSDA + U calculations for fully relaxed supercells [7,38].

Using the formulas from Table II, we find the expressions for the magnetic interactions in the PFB4 chemical configuration:

$$J_3 = (E_{4,c} - E_{4,b})/16S^2, \tag{3}$$

$$J_1 = (E_{4,b} - E_{4,a})/4S^2 + 4J_3, \tag{4}$$

$$J_2 = (E_{4,fm} - E_{4,a})/16S^2 - J_1/2. \tag{5}$$

Substituting the values of energy differences from Tables I and II into these equations, we obtain the values of the interactions given in Table III. The last row of the table shows the results for the fully relaxed lattice [7,27]. Our calculations of the total energies confirm the results of Ref. [7] [27]. But we find that the lowest energy for the second configuration corresponds to the *ferrimagnetic* type of ordering PFB2fe [39].

Table IV shows the results of the check of the quality of our mapping of LSDA + U on the Heisenberg model (1).

TABLE I. Total energy differences $E(a,U)$ (meV) for various spin structures, lattice parameters a, and Coulomb repulsion values U. The LSDA + U calculations were performed for ideal cubic perovskite structure and PFB4 chemical order (see Figs. 1–3).

Spin structure	E(4.01,4)	E(3.95,4)	E(4.01,6)
PFB4a	0	0	0
PFB4b	200	213	163
PFB4c	199	211	162
PFB4,FM	435	464	341

TABLE II. The energies of chemical and magnetic configurations for the $Pb_8Fe_4Nb_4O_{24}$ supercell, which allow one to find all exchange interactions. The calculated LSDA + U values are given for $U = 4$ eV for ion coordinates from Refs. [7,38].

Conf.	$\langle \hat{H} \rangle$	E_{calc}, meV
PFB0,FM	$E_{0,fm} = 24J_2S^2$	69
PFB0a	$E_{0,a} = -8J_2S^2$	0
PFB1, FM	$E_{1,fm} = (4J_1 + 8J_2 + 16J_3)S^2$	936
PFB1a	$E_{1,a} = (4J_1 - 8J_2 - 16J_3)S^2$	903
PFB1b	$E_{1,b} = (-4J_1 - 8J_2 + 16J_3)S^2$	437
PFB2, FM	$E_{2,fm} = (6J_1 + 12J_2)S^2$	271
PFB2a	$E_{2,a} = (-2J_1 - 4J_2)S^2$	−209
PFB2fe	$E_{2,fe} = (-6J_1 + 12J_2)S^2$	−406
PFB3fm	$E_{3,fm} = (6J_1 + 8J_2 + 8J_3)S^2$	674
PFB3a	$E_{3,a} = (-6J_1 + 8J_2 + 8J_3)S^2$	−35
PFB4, FM	$E_{4,fm} = (4J_1 + 12J_2 + 8J_3)S^2$	611
PFB4a	$E_{4,a} = (-4J_1 - 4J_2 + 8J_3)S^2$	101
PFB4b	$E_{4,b} = (-4J_2 - 8J_3)S^2$	346
PFB4c	$E_{4,c} = (-4J_2 + 8J_3)S^2$	346
PFB5, FM	$E_{5,fm} = 8(J_1 + J_2)S^2$	386
PFB5a	$E_{5,a} = 8(-J_1 + J_2)S^2$	−530

IV. DISCUSSION

A. Superexchange interaction

Our calculations strongly suggest that the magnetism of $AFe_{1/2}M_{1/2}O_3$ systems may be described by the Heisenberg model on the lattice which is obtained from the simple cubic lattice by removing half of its sites, the nearest-neighbor interaction J_1 being dominant.

The dominance of J_1 is an expected result. The magnetic interactions between Fe^{3+} ions are due to the superexchange mechanism [40], which has a local nature for $3d$-metal compounds [41,42]. The ion Fe^{3+} has d^5 electronic configuration. For this configuration, the fourth-order many-body perturbation theory expression for the superexchange via a single intervening oxygen ion (Fig. 4) may be written [43,44] in a simple form (see Appendix B for the derivation):

$$J_\alpha \approx K V_{pd\sigma,1}^2 V_{pd\sigma,2}^2 (0.475 + 0.617 \cos^2 \alpha) \tag{6}$$

$$= J_{180}(0.475 + 0.617 \cos^2 \alpha)/1.092 \tag{7}$$

$$= J_{180} \cos^2 \alpha + J_{90} \sin^2 \alpha, \tag{8}$$

where α is the Fe-O-Fe bond angle; K is given by Eq. (B7), it does not depend on the bond geometry, $V_{pd\sigma,i}$ are the Slater-Koster [45] parameters for the electron hopping integrals

TABLE III. Values of exchange parameters in the PFB4 chemical configuration.

U(eV)	a (Å)	J_1/k_B (K)	J_2/k_B (K)	J_3/k_B (K)	J_2/J_1
4	4.01	92	4.3	<0.1	0.046
6	4.01	75	2.0	−0.1	0.026
4	3.95	98	5.0	−0.3	0.051
4	∼3.95[a]	113	2.4	<0.1	0.021

[a]Fully relaxed lattice from the calculations in Ref. [7].

TABLE IV. Check of the mapping. DFT energy differences (U = 4 eV) are compared with the results for the model, Eq. (1), which assumes J_i to be *independent* on the chemical configuration.

$\Delta E/S^2$, meV	DFT	Model	Value
$(E_{5,fm} - E_{5,a})/S^2$	146.6	$16J_1$	156.5
$(E_{3,fm} - E_{3,a})/S^2$	113.4	$12J_1$	117.3
$(E_{2,fm} - E_{2,fe})/S^2$	108.3	$12J_1$	117.3
$(E_{2,fm} - E_{2,a})/S^2$	76.7	$8J_1 + 16J_2$	81.6
$(E_{2,a} - E_{2,fe})/S^2$	31.6	$4J_1 - 16J_2$	35.8
$(E_{1,fm} - E_{1,a})/S^2$	5.3	$16J_2 + 32J_3$	3.3
$(E_{1,fm} - E_{1,b})/S^2$	79.9	$8J_1 + 16J_2$	81.6
$(E_{0,fm} - E_{0,a})/S^2$	11.1	$32J_2$	6.7

between Fe and O ions, which depend only on the Fe-O bond lengths.

The dependence of the Fe-O-Fe superexchange on the square of the bond angle cosine $\cos^2\alpha$ was established for the orthoferrites $RFeO_3$ in Ref. [46] in the form given by Eq. (8). For the $RFeO_3$ family, the bond angle varies between 157° in $LaFeO_3$ to 142° in $LuFeO_3$, the Fe-O bond length being approximately constant $d \approx 2.01$ Å. Substituting the $LuFeO_3$ parameters $\cos^2\alpha \approx 0.618$ and $J/k_B \approx 48.4 \pm 2$ K into Eq. (7) we find for $J_{180}/k_B \approx 62$ K, which is comparable with our J_1 value calculated for $U = 6$. The assumption (ii) from the introduction is thus confirmed.

Our formula (6) shows also that the Fe-O-Fe superexchange depends on the Fe-O bond lengths R_i. The hopping integrals $V_{pd\sigma,i}(R_i)$ decrease with the increase of the bond length [47]. This means that the superexchange should decrease with the increase of the lattice parameter if the bond angle remains constant. The results shown in Table III follows this tendency.

We may compare our results also with Ref. [32], where the values for J_1, J_2, and fourth-neighbor J_4 exchanges were found for PFB0[$=\frac{1}{2}(111)$] and PFB5[$=\frac{1}{2}(100)$] configurations (Fig. 2). If we express the results from Table III of Ref. [32] in our notations, we obtain $-2J_1^s/k_B = J_2/k_B \approx 0.9$ K, and $-2J_2^s/k_B = J_4/k_B \approx 2.8$ K for PFB0, and $-2J_1^s/k_B = J_1/k_B \approx 42$ K, $-2J_d/k_B = J_2/k_B \approx 0.5$ K, $-2J_2^s/k_B = J_4/k_B \approx 2.8$ K for PFB5. The results of Ref. [32] confirm the dominance of J_1 nearest-neighbor Fe-O-Fe interaction. The absolute value of the interaction is smaller, but we should take into account that the authors of Ref. [32] have used the $U = 9$ eV value in those calculations. Note that they obtained $J_1/k_B \approx 50$ K for $LaFeO_3$, which is slightly smaller than the experimental value [11] 59 K derived from $T_N = 740$ K using high-temperature expansion.

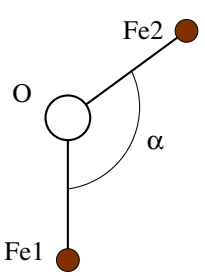

FIG. 4. (Color online) The geometry of the Fe_1-O-Fe_2 superexchange path.

B. Collective magnetic properties

The way half of the sites of the simple cubic lattice are occupied by the interacting Fe spins determines the magnetic properties of the system. In this work, we model the disorderd system by the $2 \times 2 \times 2$ supercell periodic lattice. If we take into account only nearest-neighbor interaction J_1, then magnetic ions form three-dimensional lattice only in PFB2 and PFB3 configurations (Fig. 2). Thus, only these configurations may possess a magnetic long-range order at nonzero temperature. Other configurations have lower dimensionalities and thus have no ordering at finite temperatures. Actually, small next-nearest-neighbor interactions (like J_2, J_3) will ensure the ordering, but the temperature will be substantially lower (see below the consideration of the PFB5 structure in Section IV C).

The simplest molecular field approach gives for the ferrimagnetic ordering temperature (see Appendix C for the details) of the PFB2fe configuration,

$$T_{2fe} = J_1 2\sqrt{3}\frac{S(S+1)}{3k_B} \approx 10.1 J_1, \tag{9}$$

and for the antiferromagnetic ordering temperature of PFB3a configuration,

$$T_{3a} = J_1 2\frac{S(S+1)}{3k_B}\sqrt{\frac{3+\sqrt{5}}{2}} \approx 9.44 J_1. \tag{10}$$

Substitution of the calculated J_1 value gives $T_{2fe} \approx$ 933(758) K, $T_{3a} \approx$ 872(708) K for U= 4(6) eV. We should have in mind that the molecular field theory overestimates the transition temperature by the factor ~1.5 for cubic lattices and this factor may increase for the structures with the number of neighbors less than 6. Indeed, a more accurate estimate may be derived from the high-temperature expansion of the magnetic susceptibility χ. In Ref. [39], we have applied the method and the program package for the eighth-order high-temperature expansion for a general Heisenberg model with up to four different exchange parameters J_1, J_2, J_3, J_4 presented recently in Refs. [48,49]. The temperature for the transition into the ferrimagnetically ordered phase $T_{fe,\mathrm{HTE}}$ is defined as the point where $\chi^{-1}(T_{fe}) = 0$. We have obtained $T_{fe,\mathrm{HTE}} \approx 5.6 J_1 \approx$ 517(420) for $U = 4(6)$ eV (see the details in Ref. [39]).

The ferrimagnetism in PFB2 chemical order has rather unusual nature. In many cases, the ferrimagnetism is due to different spin values of ions occupying different antiferromagnetically coupled magnetic sublattices. Another possibility is realized, e.g., in the yttrium iron garnet $Y_3Fe_5O_{12}$ and related compounds. There, all Fe ions have equal spins $S = 5/2$, but the lattice has two kinds of Fe positions, and the number of Fe sites in antiparallel sublattices is different [50,51]. So, the ferrimagnetism may have a purely geometrical origin [52]. This is the case for the magnetic ground state of the PFB2 chemically ordered lattice [39].

We understand that $2 \times 2 \times 2$ supercell periodic lattice is a rather poor approximation to the disordered system. Nevertheless, it is instructive to estimate the probabilities to find different chemical configurations PFBn (see Figs. 2 and 3 of Ref. [7]). If the system is totally disordered, i.e., if Fe

TABLE V. The Curie-Weiss $\Theta_{CW,0}$ and calculated transition $T_I = -\Theta_{CW,0}/5.76$ temperatures for 1:1 ordered systems. DFT calculations and experimental results. The temperature of observed susceptibility anomaly T_{max} is shown for two compounds.

U, eV	$\Theta_{CW,0}$, K	T_I, K	T_{max}, K
4	−151	26	
6	−70	12	
$Sr(Fe_{1/2}Sb_{1/2})O_3$[a]	−221	38	36
$Ca(Fe_{1/2}Sb_{1/2})O_3$[b]	−89	15	17

[a]Reference [24].
[b]Reference [23].

and M ions randomly occupy B sites of the perovskite lattice [assumption (i) of the introduction], we have $C_8^4 = 70$ ways to distribute Fe ions over eight vertices of the cube, every configuration being equivalent to the one of that depicted in Fig. 2. We will meet 2 times the configuration PFB0, 6 times PFB1 and PFB5 configurations, 8 times PFB2, and 24 times PFB3 and PFB4 configurations $2 + 2 \times 6 + 8 + 2 \times 24 = 70$. So, in the case of random distribution, the probability to meet the PFB2 configuration is $P_2 = 8/70 \approx 0.11$, and to meet the PFB3 configuration is $P_3 = 24/70 \approx 0.34$. Thus the magnetic properties of an $AFe_{1/2}M_{1/2}O_3$ compound will be dominated by the PFB3 configuration. So, within our simple model of disorder the transition temperature would be several hundred K. As we have mentioned in the introduction, more sophisticated treatment of the disorder results in $T_N \sim 300$ K [21,22]. Evidently, the assumption (i) is in contradiction with the observed values of the transition and Curi-Weiss temperatures.

The distribution of Fe and M ions over B sites depends on the ratio of ionic radii of Fe and M metal ions, the growth condition of the sample, etc. When the radius of M^{5+} ion is larger than that of Fe^{3+}, the ordered PFB0 configuration becomes most probable [7]. This is often the case for M = Sb [23,53]. For such 1:1 ordered systems, magnetic Fe^{3+} ions form a regular face-centered cubic sublattice with interaction J_2 between nearest spins in the sublattice. The Curie-Weiss temperature is $\Theta_{CW,0} = 4S(S+1)J_2/k_B$. The magnetic ground state of such Heisenberg lattice is the so-called I-type order, which is denoted as PFB0a in Fig. 2. The transition temperature was studied in Ref. [54] using high-temperature series expansion. It occurs as spin independent and equals $T_I \approx -\Theta_{CW,0}/5.76$. Table V compares the calculated values of T_I with the temperature T_{max} of the magnetic susceptibility anomaly observed in 1:1 ordered $AFe_{1/2}M_{1/2}O_3$ compounds.

C. Magnetism of the $PbFe_{1/2}M_{1/2}O_3$ compounds

The total energies of various chemical configurations (see Fig. 2) of Fe in a $2 \times 2 \times 2$ supercell of $PbFe_{1/2}M_{1/2}O_3$ (M = Nb, Ta, Sb) were calculated in Ref. [7] using the LSDA + U functional. For the PFN and $PbFe_{1/2}Ta_{1/2}O_3$ (M = Nb, Ta) compounds, the layered PFB5a configuration has the lowest energy, in contrast to $PbFe_{1/2}Sb_{1/2}O_3$, where the PFB0 1:1 chemically ordered configuration is most favorable [27] (see also Table II). The PFN and $PbFe_{1/2}Ta_{1/2}O_3$ compounds are especially interesting because they are multiferroics and exhibit ferroelectric transition ($T_C \approx 380$, 270 K for M = Nb, Ta) in addition to antiferromagnetic transition. As we have mentioned in the introduction, the peculiarity of magnetic properties of these two compounds is that those Néel temperature $T_N \sim 150$ K is much higher than the transition temperature for other double perovskites. A layered Heisenberg model with the nearest-neighbor interaction J_1 within the layer and an interlayer interaction $J_\perp$ was thoroughly studied in the past (see Ref. [55] and references therein). It was established that the transition temperature has logarithmic dependence on the $J_\perp/J_1$ ratio,

$$\frac{T_N}{T_{N,sc}} \approx \frac{1}{1 - k\ln(J_\perp/J_1)}, \tag{11}$$

where $T_{N,sc}$ is the transition temperature for the G-type antiferromagnetic ordering of the simple cubic lattice ($J_\perp = J_1$), and $k \approx 1/3$. Equation (11) was found to work in the wide range of values $0.001 \leqslant J_\perp/J_1 \leqslant 1$ [55,56], it gives $T_N/T_{N,sc} \approx 0.30$, 0.39, 0.57 for $J_\perp/J_1 = 0.001$, 0.01, 0.1, respectively. Taking $T_{N,sc} \sim 600$ K, we obtain reasonable values for $T_N \approx 180$, 234, 342, respectively, if we assume that PFN and $PbFe_{1/2}Ta_{1/2}O_3$ have the totally ordered layered structure.

In reality, both compounds are disordered and the results of the supercell calculations indicate only what kind of *short-range* chemical order is more favorable. Below T_N, the neutron diffraction studies [4,57,58] reveal a G-type antiferromagnetic order with magnetic moments $\mu \approx 2.8\mu_B$ sitting at *every* site of the simple cubic lattice. It is clear that this is an averaged picture with "half of Fe^{3+} ion" in every site of the B sublattice of the structure. The value of μ is about half of the value expected for the Fe^{3+} ion $\mu_{Fe} = 5\mu_B$.

In contrast to neutron diffraction, local probe methods such as nuclear magnetic resonance (NMR) and Mossbauer spectroscopy provide local structure information. In this respect, we can mention ^{17}O NMR data [25] which may confirm our theoretical prediction that the PFB5 configuration gives major contribution to the antiferromagnetic ground state of PFN or $PbFe_{1/2}Ta_{1/2}O_3$. Indeed, the ^{17}O NMR spectrum consists of two distinct components: narrow and very broad lines. One can see from Fig. 1 that each O ion connects only two cations forming three different pathways along ⟨100⟩ cubic directions: Fe-O-Fe, Fe-O-Nb, and Nb-O-Nb. The first two configurations are responsible for the broad component in the ^{17}O NMR spectrum as the O nucleus is closely adjacent to the magnetic Fe^{3+} ion. The last configuration does not contain magnetic ions therefore is responsible for the narrow component in the NMR spectrum. Among all chemical configurations shown in Fig. 2, the PFB5 configuration has the largest number of nonmagnetic Nb-O-Nb chains. Assuming, for example, random distribution of Fe and Nb ions we have relative weight of the Nb-O-Nb pathways only 0.19, while the NMR data predicts 2–2.5 times larger value. This suggests that the layered PFB5 chemical configuration can dominate among other chemical ordering. The nonrandom distribution of magnetic and nonmagnetic cations in PFN is also supported by ^{93}Nb NMR measurements [6]. The NMR data have been interpreted in a model which assumes existence of Fe rich, Nb poor and Fe poor, Nb rich regions in PFN.

Table II shows that the PFB2fe configuration has the total energy, which is close to the lowest PFB5 configuration. This is the case also for $PbFe_{1/2}Ta_{1/2}O_3$ and $PbFe_{1/2}Sb_{1/2}O_3$ [27]. A sample of a disordered double perovskite compound may contain some regions with PFB2 chemical order. In the ground state, such a region possesses the moment $\mu_g = N_c\mu_c$, where N_c is the number of supercells in the region; $\mu_c = 10\mu_B$ is the moment of the supercell. Large moment of the region will persist for $T < T_{2fe}$. Therefore, it cannot be excluded that such regions exist in the systems $PbFe_{1/2}Ta_{1/2}O_3/PbZr_xTi_{1-x}O_3$ [29,30], $PFN/PbZr_xTi_{1-x}O_3$ [28], and $PbFe_{2/3}W_{1/3}O_3/PbZr_xTi_{1-x}O_3$ [31] and are responsible for large room-temperature magnetic response and magnetoelectric coupling despite that the long-range magnetic order establishes far below the room temperatures.

V. CONCLUSION

Based on LSDA + U calculations, we have found that $AFe_{1/2}M_{1/2}O_3$ double perovskite compounds may be described by the antiferromagnetic $J_1 - J_2$ Heisenberg model on the lattice, which is obtained from the simple cubic lattice by removing half of its sites. The dominant magnetic interaction is the Fe-O-Fe superexchange J_1 between Fe^{3+} (S = 5/2) ions occupying nearest-neighbor positions within the B sublattice of the ABO_3 perovskite structure. The next-nearest-neighbor interaction J_2 which corresponds to sites separated by the face diagonal of the perovskite unit cell is much smaller. The estimated values of the exchange parameters are close to the values reported for Fe-based perovskites $RFeO_3$, where all octahedral sites are occupied by Fe ions. The distribution of Fe^{3+} and M^{5+} ions over B sites of the perovskite lattice determine the magnetic properties of the double perovskites. Our results suggest that the distribution is *not* random. The typical value of the magnetic transition temperature $T_N \sim 25$ K in most of the paraelectric double perovskite compounds allows one to conclude that the probability to find there a nearest-neighbor pair of Fe (interacting with the J_1 exchange value) is suppressed compared to the probability to find the next-nearest pair, and the magnetic energy scale is determined by J_2. In accord with Ref. [7], we argue that two multiferroic compounds $PbFe_{1/2}Nb_{1/2}O_3$ and $PbFe_{1/2}Ta_{1/2}O_3$ ($T_N \sim 150$ K) have predominantly layered PFB5 (see Fig. 2) short-range ordering where the B sublattice is formed by alternating Fe and M(=Nb or Ta) planes.

We have also found that Fe ion in double perovskites may form a subnanosized superstructure (PFB2 chemical order in Fig. 2) having the room-temperature *ferrimagnetic* order. Such ferrimagnetism of geometrical origin [52] may represent an interesting alternative to the room-temperature ferromagnetism in wide-gap semiconductors, which is in the focus of recent studies. Formation of the PFB2 superstructure in ferroelectric double perovskites will lead to the room-temperature multiferroism where ferroelectric- and ferrimagnetic-type order can coexist, at least at a nanoscale level. Recent observations of the room-temperature multiferroism in complex systems on the base of the double perovskites [28–31] are possibly provided by nanoregions of the ferrimagnetic PFB2 superstructure rather than by simple local clustering of Fe ions as this will lead only to an increase of Neel temperature.

ACKNOWLEDGMENTS

The authors thank M. D. Kuz'min for very useful discussions, S. A. Prosandeev for providing the details on numerical calculations in Ref. [7], U. Nitzsche and K. Koepernik for technical assistance, and the IFW Dresden (Germany) for the use of their computer facilities. The project GACR 13-11473S is acknowledged.

APPENDIX A: DETAIL OF THE LSDA + U CALCULATIONS

Total and projected densities of states are shown in Fig. 5. As expected, the largest spin splitting occurs for Fe 3d states. Table VI shows the values of magnetic moments localized on the Fe ions. They are close to the isolated Fe^{3+} ion value $5\mu_B$. In the ground-state PFB4a configuration, the polarization does not exceed $0.03\mu_B$ for oxygen ions, and $0.04\mu_B$ for Nb ions. In the ferromagnetic state, the polarization of some oxygens and Nb ions reaches $0.14\mu_B$ and $0.12\mu_B$, respectively. We see that

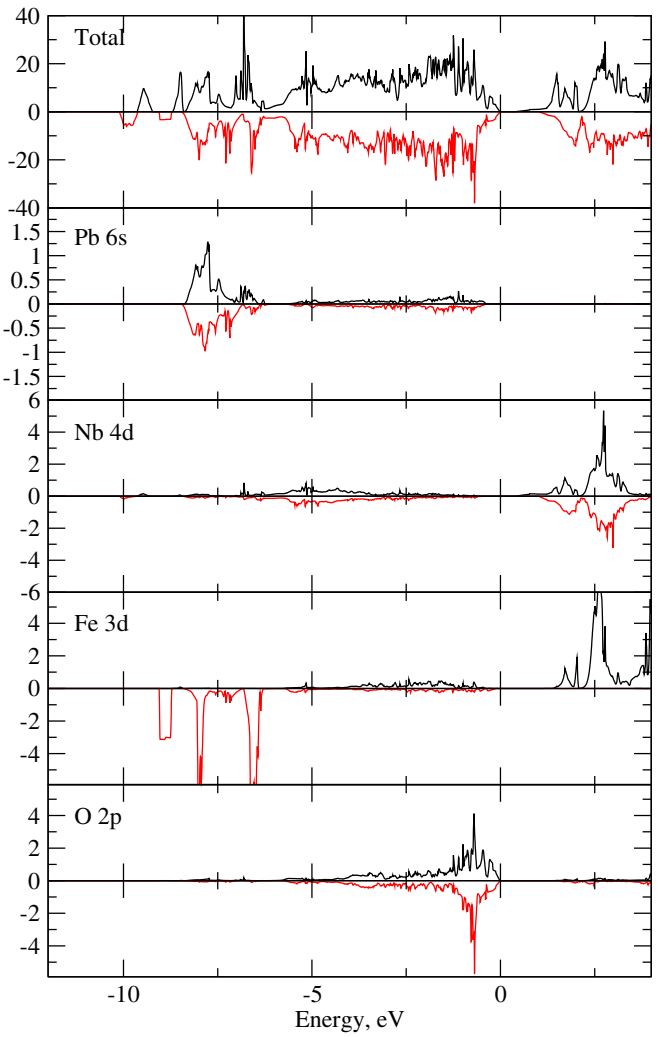

FIG. 5. (Color online) Spin-resolved total density of states (upper panel) for the PFB4a structure, $U = 6$ eV. Other panels show representative densities of states projected onto the basis functions (one for every ion sort), which maximally contribute to the total density of state near the Fermi level.

TABLE VI. The magnetic moments (in the units of Bohr magneton μ_B) localized on different Fe ions of the PFB4 chemical configuration in various magnetic states depicted in Figs. 2 and 3.

	U(eV)	a (Å)	Fe1	Fe2	Fe3	Fe4
a	4	4.01	4.45	4.45	−4.39	−4.52
	6	4.01	4.77	4.77	−4.71	−4.85
	4	3.95	4.49	4.49	−4.42	−4.56
	4	∼3.95[a]	4.43	4.43	−4.35	−4.45
b	4	4.01	4.49	−4.45	4.43	−4.51
	6	4.01	4.79	−4.77	4.73	−4.85
	4	3.95	4.52	−4.49	4.45	−4.55
	4	∼3.95[a]	4.49	−4.43	4.41	−4.45
FM	4	4.01	4.50	4.50	4.48	4.50
	6	4.01	4.80	4.80	4.75	4.85
	4	3.95	4.53	4.53	4.49	4.54
	4	∼3.95[a]	4.50	4.49	4.47	4.45

[a]Fully relaxed lattice from the calculations in Ref. [7].

the localized moment description of the magnetism in PFN by the model Hamiltonian (1) is adequate.

APPENDIX B: THREE CENTER CATION-ANION-CATION MODEL

Here we will calculate the superexchange for the case when it is mediated by one anion where the CF splitting will be neglected. Then we choose the coordinate system having the anion in the origin, and the vector radii of the cations are

$$\mathbf{R}_1 = (0,0,-1)\,R_1,$$
$$\mathbf{R}_2 = (\sin\alpha,0,-\cos\alpha)\,R_2,$$

where α is the angle between bonds (Fig. 4). A general fourth-order many-body perturbation theory expression for the superexchange between two ions in the d^5 configuration reads [cf. Eqs. (9) and (10) of Ref. [44]]

$$J = -\frac{1}{2S^2\Delta_{\text{eff}}^2}\left(\frac{r^2}{U_{\text{eff}}} + \frac{2}{2\Delta_{\text{eff}} + U_p}\right) E_{\beta\beta}, \tag{B1}$$

where

$$E_{\beta\beta} = \sum_{m,m',n,n'} t_{1,m,\beta,n}t_{2,m',\beta,n}t_{1,m,\beta,n'}t_{2,m',\beta,n'}, \tag{B2}$$

$$U_{\text{eff}} = U_d + 4J_H, \tag{B3}$$

$$\Delta_{\text{eff}} = \Delta + 28J_H/9. \tag{B4}$$

The d ions are assumed to be in the high-spin state ($S = 5/2$), U_d (U_p) is the Coulomb repulsion between two fermions on the same $d(p)$ orbital, $J_H \equiv \frac{5}{2}B + C$ is the Hund exchange in the d shell expressed in terms of Racah parameters, and Δ is the charge transfer energy (see Ref. [44] for the discussion of the approximations behind Eq. (B1), and the description of the realistic many-body $p-d$ Hamiltonian). According to the Harrison model [47], the hopping $t_{\alpha,m,\beta,n}$ between the mth d function of metal ion $\alpha = 1,2$ and the nth p function of ligand β is expressed via direction cosines l,m,n of the vector $\mathbf{R}_\beta - \mathbf{R}_\alpha$, and two Slater-Koster [45] parameters $V_{pd\sigma}(R), V_{pd\pi}(R)$, which depend on sorts of metal ion and on the distance $R = |\mathbf{R}_\beta - \mathbf{R}_\alpha|$; $r \approx 0.8$ is a reduction factor that is caused by dependence of the hoppings on the number of $3d$ electrons.

In the case of the single ligand, the index β may be dropped, and it is convenient to write

$$E \equiv \sum_{n,n'}\sum_{m,m'} t_{1,m,n}t_{2,m',n}t_{1,m,n'}t_{2,m',n'}$$
$$= \sum_{n,n'}\sum_{m} t_{1,m,n}t_{1,m,n'}\sum_{m'} t_{2,m',n}t_{2,m',n'}.$$

The Slater-Koster table [45,47] gives for the first transition metal-anion pair,

$$t_{1zx,x} = t_{1zy,y} = -V_{pd\pi,1},$$
$$t_{1z^2,z} = -V_{pd\sigma,1},$$

other hoppings are zero. So

$$\sum_m t_{1,m,n}t_{1,m,n'} = \delta_{nn'}\sum_m t_{1,m,n}^2 \equiv \delta_{nn'}T_{1n},$$
$$T_{1x} = T_{1y} = V_{pd\pi,1}^2, \quad T_{1z} = V_{pd\sigma,1}^2,$$

then

$$E = \sum_{n,n'}\delta_{nn'}T_{1n}\sum_{m'} t_{2,m',n}t_{2,m',n'} = \sum_n T_{1n}T_{2n},$$
$$T_{2n} \equiv \sum_{m'} t_{2,m',n}^2.$$

For the second anion-TMI pair the hoppings are given in Tables VII and VIII. This gives us

$$T_{2x} = \sin^2\alpha V_{pd\sigma,2}^2 + \cos^2\alpha V_{pd\pi,2}^2,$$
$$T_{2y} = V_{pd\pi,2}^2,$$
$$T_{2z} = \cos^2\alpha V_{pd\sigma,2}^2 + \sin^2\alpha V_{pd\pi,2}^2.$$

And we obtain

$$E = V_{pd\pi,1}^2(T_{2x} + T_{2y}) + V_{pd\sigma,1}^2T_{2z}$$
$$= V_{pd\pi,1}^2\left[\sin^2\alpha V_{pd\sigma,2}^2 + (1+\cos^2\alpha)V_{pd\pi,2}^2\right]$$
$$+ V_{pd\sigma,1}^2\left(\cos^2\alpha V_{pd\sigma,2}^2 + \sin^2\alpha V_{pd\pi,2}^2\right) \tag{B5}$$

TABLE VII. Hoppings $t_{2m'n'}$ between t_{2g} orbitals and ligand p functions.

n\m	xy	yz	zx
x	0	0	$-\cos\alpha\left[\sqrt{3}\sin^2\alpha V_{pd\sigma} + (1-2\sin^2\alpha)V_{pd\pi}\right]$
y	$\sin\alpha V_{pd\pi}$	$-\cos\alpha V_{pd\pi}$	0
z	0	0	$-\sin\alpha\left[\sqrt{3}\cos^2\alpha V_{pd\sigma} + (1-2\cos^2\alpha)V_{pd\pi}\right]$

TABLE VIII. Hoppings $t_{2m'n'}$ between e_g orbitals and ligand p functions.

n\m	x^2-y^2	z^2
x	$\frac{\sqrt{3}}{2}\sin^3\alpha V_{pd\sigma}+\sin\alpha(1-\sin^2\alpha)V_{pd\pi}$	$\sin\alpha\left[\left(\cos^2\alpha-\frac{\sin^2\alpha}{2}\right)V_{pd\sigma}-\sqrt{3}\cos^2\alpha V_{pd\pi}\right]$
y	0	0
z	$-\cos\alpha\left[\frac{\sqrt{3}}{2}\sin^2\alpha V_{pd\sigma}-\sin^2\alpha V_{pd\pi}\right]$	$-\cos\alpha\left[\left(\cos^2\alpha-\frac{\sin^2\alpha}{2}\right)V_{pd\sigma}+\sqrt{3}\sin^2\alpha V_{pd\pi}\right]$

$$= V_{pd\sigma,1}^2 V_{pd\sigma,2}^2 \frac{1+2\tau^2+(\tau^2-1)^2\cos^2\alpha}{\tau^4}$$

$$\approx V_{pd\sigma,1}^2 V_{pd\sigma,2}^2 (0.475+0.617\cos^2\alpha). \quad \text{(B6)}$$

In the last equality we have introduced the ratio $\tau \equiv V_{pd\sigma}/V_{pd\pi} \approx -2.16$ [47].

Finally, we obtain Eq. (6) of the main text with

$$K = \frac{r^2}{U_{\text{eff}}} + \frac{2}{2\Delta_{\text{eff}}+U_p}. \quad \text{(B7)}$$

APPENDIX C: TRANSITION TEMPERATURE

Here we give the derivation of Eqs. (9) and (10) for transition temperatures within the molecular field approximation (see, e.g., Ref. [59]).

In the PFB2fe configuration we have two sublattices: Fe1 with spin-up and Fe2 with spin-down. In a supercell, one of the ions belongs to the sublattice Fe1 and three to the sublattice Fe2. The molecular fields acting on the magnetic moments are

$$H_2 = -\lambda M_1, \quad \text{(C1)}$$

$$H_1 = -\lambda M_2, \quad \text{(C2)}$$

$$\lambda \equiv \frac{2J_1}{N\mu^2}, \quad \text{(C3)}$$

where N is the number of supercells, $\mu = g\mu_B$, g is the g factor of the Fe^{3+} ion, μ_B is the Bohr magneton, M_1 (M_2) is the magnetization of the Fe1(Fe2) sublattice. The magnetization, in its turn, is defined by the molecular field,

$$M_s = Nn_s\mu S B_S\left(\frac{\mu S}{k_B T}H_s\right) \quad \text{(C4)}$$

$$\approx \frac{C_s}{T}H_s, \quad \text{(C5)}$$

where $s = 1,2$, n_s is the number of ions in the supercell that belongs to the sublattice s, $n_2 = 3n_1 = 3$,

$$C_s = \frac{Nn_s\mu^2 S(S+1)}{3k_B}$$

is the corresponding Curie constant, $B_L(x) \equiv [(2L+1)/2L]\coth[(2L+1)x/2L] - (1/2L)\coth x/2L$ is the Brillouin function. The equality (C5) follows from the expansion $B_L(x) \approx (L+1)x/3L$, which is valid for small x. Substituting the value of the molecular field from Eqs. (C1) and (C2) into Eq. (C5), we obtain the system of equations for the sublattice magnetizations in the absence of the external field,

$$\begin{aligned} TM_1 + C_1\lambda M_2 &= 0, \\ C_2\lambda M_1 + TM_2 &= 0, \end{aligned} \quad \text{(C6)}$$

which has trivial solution $M_1 = M_2 = 0$ above the transition temperature $T > T_{2fe}$. Nonzero values of the magnetizations becomes possible if the determinant of the coefficients of M_1 and M_2 is zero. This condition yields

$$(T_{fe})^2 = C_1C_2\left(\frac{2J_1}{N\mu^2}\right)^2, \quad \text{(C7)}$$

and we obtain Eq. (9). At lower temperatures $T < T_{fe}$, the system becomes nonlinear as the argument of the Brillouin function grows.

The calculation for PFB3a magnetic ordering is more involved. We have four sublattices shown in Fig. 2, Curie constants are equal $C = N\mu^2 S(S+1)/3k_B$, and we have four equations,

$$\begin{aligned} TM_{B,1} &= CH_{B,1} = -C\lambda(M_{A,1}+M_{A,2}), \\ TM_{B,2} &= CH_{B,2} = -C\lambda M_{A,1}, \\ TM_{A,1} &= CH_{A,1} = -C\lambda(M_{B,1}+M_{B,2}), \\ TM_{A,2} &= CH_{A,2} = -C\lambda M_{B,1}. \end{aligned} \quad \text{(C8)}$$

Again, at the transition temperature, the determinant of the coefficients should vanish. This gives a biquadratic equation,

$$T^4 - 3(C\lambda)^2T^2 + (C\lambda)^4 = 0. \quad \text{(C9)}$$

The transition temperature is given by the largest positive root of Eq. (C9), as it corresponds to the temperature where the nontrivial solution appears when we approach the transition from the paramagnetic side. We thus obtain Eq. (10).

[1] G. Smolenskii and V. A. Loffe, Communication No. 71 (Colloque International du Magnetisme, Grenoble, 1958).

[2] V. Bokov, I. Myl'nikova, and G. A. Smolenskii, Sov. Phys. JETP **15**, 447 (1962).

[3] I. P. Raevski, S. P. Kubrin, S. I. Raevskaya, V. V. Titov, D. A. Sarychev, M. A. Malitskaya, I. N. Zakharchenko, and S. A. Prosandeev, Phys. Rev. B **80**, 024108 (2009).

[4] G. M. Rotaru, B. Roessli, A. Amato, S. N. Gvasaliya, C. Mudry, S. G. Lushnikov, and T. A. Shaplygina, Phys. Rev. B **79**, 184430 (2009).

[5] W. Kleemann, V. V. Shvartsman, P. Borisov, and A. Kania, Phys. Rev. Lett. **105**, 257202 (2010).

[6] V. Laguta, J. Rosa, L. Jastrabik, R. Blinc, P. Cevc, B. Zalar, M. Remskar, S. Raevskaya, and I. Raevski, Mater. Res. Bull. **45**, 1720 (2010).

[7] I. P. Raevski, S. P. Kubrin, S. I. Raevskaya, D. A. Sarychev, S. A. Prosandeev, and M. A. Malitskaya, Phys. Rev. B **85**, 224412 (2012).

[8] V. V. Laguta, M. D. Glinchuk, M. Maryško, R. O. Kuzian, S. A. Prosandeev, S. I. Raevskaya, V. G. Smotrakov, V. V. Eremkin, and I. P. Raevski, Phys. Rev. B **87**, 064403 (2013).

[9] S. Kubrin, Ph.D thesis, Southern Federal University, Rostov on Don 344090, Russia, 2009.

[10] D. Treves, J. Appl. Phys. **36**, 1033 (1965).

[11] M. Eibschütz, S. Shtrikman, and D. Treves, Phys. Rev. **156**, 562 (1967).

[12] Z. V. Gabbasova, M. D. Kuz'min, A. K. Zvezdin, I. S. Dubenko, V. A. Murashov, D. N. Rakov, and I. B. Krynetsky, Phys. Lett. A **158**, 491 (1991).

[13] G. Gorodetsky, J. Phys. Chem. Solids **30**, 1745 (1969).

[14] S. M. Shapiro, J. D. Axe, and J. P. Remeika, Phys. Rev. B **10**, 2014 (1974).

[15] A. Gukasov, U. Steigenberger, S. Barilo, and S. Guretskii, Physica B: Condensed Matter **234**, 760 (1997).

[16] O. Delaire, M. B. Stone, J. Ma, A. Huq, D. Gout, C. Brown, K. F. Wang, and Z. F. Ren, Phys. Rev. B **85**, 064405 (2012).

[17] R. J. McQueeney, J.-Q. Yan, S. Chang, and J. Ma, Phys. Rev. B **78**, 184417 (2008).

[18] The J_1, J_2 values for the orthoferrites $YFeO_3$ and $LuFeO_3$ were obtained in Ref. [13] from the high-temperature analysis of the paramagnetic susceptibility. In our notations, they are $J_1/k_B = 54.4 \pm 2$ K, $J_2/k_B = 2.4 \pm 0.4$ K, for $YFeO_3$, and $J_1/k_B = 48.4 \pm 2$ K, $J_2/k_B = 2 \pm 0.2$ K for $LuFeO_3$. Note that the author of Ref. [13] uses another definition of the exchange, and we have multiplied his values by the factor (-2) for the comparison with our values. The inelastic neutron scattering studies [14–17] shows that J_1, J_2 have almost the same values for all the $RFeO_3$ family, the small variations being due to the Fe-O-Fe angle variations [46].

[19] G. D'Ariano and F. Borsa, Phys. Rev. B **26**, 6215 (1982).

[20] D. J. Breed, K. Gilijamse, J. W. E. Sterkenburg, and A. R. Miedema, J. Appl. Phys. **41**, 1267 (1970).

[21] R. B. Stinchcombe, J. Phys. C **12**, 4533 (1979).

[22] D. Kumar, R. B. Pandey, and M. Barma, Phys. Rev. B **23**, 2269 (1981).

[23] P. D. Battle, T. Gibb, A. Herod, S.-H. Kim, and P. Munns, J. Mater. Chem. **5**, 865 (1995).

[24] P. D. Battle, T. Gibb, A. Herod, and J. Hodges, J. Mater. Chem. **5**, 75 (1995).

[25] R. Blinc, V. V. Laguta, B. Zalar, B. Zupančič, and M. Itoh, J. Appl. Phys. **104**, 084105 (2008).

[26] B.-L. Gu, H. Gui, Z.-R. Liu, and X.-W. Zhang, J. Appl. Phys. **85**, 2408 (1999).

[27] Note that in Ref. [7], rows 2 and 4 of Table II are interchanged compared with Fig. 3. Actually, the PFB2 configuration has the energy close to the PFB5 one.

[28] D. A. Sanchez, N. Ortega, A. Kumar, G. Sreenivasulu, R. S. Katiyar, J. F. Scott, D. M. Evans, M. Arredondo-Arechavala, A. Schilling, and J. M. Gregg, J. Appl. Phys. **113**, 074105 (2013).

[29] D. A. Sanchez, N. Ortega, A. Kumar, R. Roque-Malherbe, R. Polanco, J. F. Scott, and R. S. Katiyar, AIP Advances **1**, 042169 (2011).

[30] D. Evans, A. Schilling, A. Kumar, D. Sanchez, N. Ortega, M. Arredondo, R. Katiyar, J. Gregg, and J. Scott, Nat. Commun. **4**, 1534 (2013).

[31] A. Kumar, G. L. Sharma, R. S. Katiyar, R. Pirc, R. Blinc, and J. F. Scott, J. Phys.: Condens. Matter **21**, 382204 (2009).

[32] N. Lampis, C. Franchini, G. Satta, A. Geddo-Lehmann, and S. Massidda, Phys. Rev. B **69**, 064412 (2004).

[33] Computer code FPLO-9.00-34 [improved version of the original FPLO code by K. Koepernik and H. Eschrig, Phys. Rev. B **59**, 1743 (1999)]; [http://www.FPLO.de].

[34] J. P. Perdew and Y. Wang, Phys. Rev. B **45**, 13244 (1992).

[35] H. Eschrig, K. Koepernik, and I. Chaplygin, J. Solid State Chem. **176**, 482 (2003).

[36] M. T. Czyzyk and G. A. Sawatzky, Phys. Rev. B **49**, 14211 (1994).

[37] Y. Tanabe and S. Sugano, J. Phys. Soc. Jpn. **9**, 766 (1954).

[38] Courtesy of the authors of Ref. [7].

[39] R. O. Kuzian, V. V. Laguta, and J. Richter, arXiv:1310.8079 [cond-mat.mtrl-sci].

[40] P. W. Anderson, *Solid State Physics*, edited by F. Seitz and D. Turnbull, Vol. 14 (Academic Press, Waltham, 1963), pp. 99–214.

[41] B. E. Larson, K. C. Hass, H. Ehrenreich, and A. E. Carlsson, Phys. Rev. B **37**, 4137 (1988).

[42] B. E. Larson and H. Ehrenreich, Phys. Rev. B **39**, 1747 (1989).

[43] R. O. Kuzian, V. V. Laguta, A.-M. Dar, I. V. Kondakova, M. Marysko, L. Raymond, E. P. Garmash, V. N. Pavlikov, A. Tkach, P. M. Vilarinho, and R. Hayn, EPL (Europhys. Lett.) **92**, 17007 (2010).

[44] R. O. Kuzian, A. M. Daré, A. Savoyant, S. D'Ambrosio, and A. Stepanov, Phys. Rev. B **84**, 165207 (2011).

[45] J. C. Slater and G. F. Koster, Phys. Rev. **94**, 1498 (1954).

[46] C. Boekema, F. Van der Waude, and G. A. Sawatzky, Int. J. Magnetism **3**, 341 (1972).

[47] W. A. Harrison, *Electronic Structure and the Properties of Solids* (Freeman, San Francisco, 1980).

[48] H.-J. Schmidt, A. Lohmann, and J. Richter, Phys. Rev. B **84**, 104443 (2011).

[49] We have used the 2011-09-23 version of the HTE package available at [http://www.uni-magdeburg.de/jschulen/HTE].

[50] S. Geller and M. Gilleo, Journal of Physics and Chemistry of Solids **3**, 30 (1957).

[51] V. Cherepanov, I. Kolokolov, and V. L'vov, Phys. Rep. **229**, 81 (1993).

[52] E. Lieb and D. Mattis, J. Math. Phys. **3**, 749 (1962).

[53] I. Raevskii, D. Sarychev, S. Bryugeman, L. Reznichenko, L. Shilkina, O. Razumovskaya, V. Nikolaev, N. Vyshatko, and A. Salak, Crystallogr. Rep. **47**, 1012 (2002).

[54] K. Pirnie, P. Wood, and J. Eve, Mol. Phys. **11**, 551 (1966).

[55] I. Juhász Junger, D. Ihle, and J. Richter, Phys. Rev. B **80**, 064425 (2009).

[56] C. Yasuda, S. Todo, K. Hukushima, F. Alet, M. Keller, M. Troyer, and H. Takayama, Phys. Rev. Lett. **94**, 217201 (2005).

[57] J. Pietrzak, A. Maryanowska, and J. Leciejewicz, Physica Status Solidi (a) **65**, K79 (1981).

[58] S. A. Ivanov, R. Tellgren, H. Rundlof, N. W. Thomas, and S. Ananta, J. Phys.: Condens. Matter **12**, 2393 (2000).

[59] A. H. Morrish, *Physical Principles of Magnetism* (R.E. Krieger Publishing Company, Huntington, 1980).